IPSJ Transactions on Computer Vision and Applications Vol.7 41–49 (May 2015)

[DOI: 10.2197/ipsjtcva.7.41]

Research Paper

Computer Simulation of Color Confusion for Dichromats in Video Device Gamut under Proportionality Law

Hiroshi Fukuda[1,a)] Shintaro Hara[2,b)] Ken Asakawa[1,c)] Hitoshi Ishikawa[1,d)]
Makoto Noshiro[1,e)] Mituaki Katuya[3,f)]

Received: September 9, 2014, Accepted: February 24, 2015, Released: May 7, 2015

Abstract: Dichromats are color-blind persons missing one of the three cone systems. We consider a computer simulation of color confusion for dichromats for any colors on any video device, which transforms color in each pixel into a representative color among the set of its confusion colors. As a guiding principle of the simulation we adopt the proportionality law between the pre-transformed and post-transformed colors, which ensures that the same colors are not transformed to two or more different colors apart from intensity. We show that such a simulation algorithm with the proportionality law is unique for the video displays whose projected gamut onto the plane perpendicular to the color confusion axis in the LMS space is hexagon. Almost all video display including sRGB satisfy this condition and we demonstrate this unique simulation in sRGB video display. As a corollary we show that it is impossible to build an appropriate algorithm if we demand the additivity law, which is mathematically stronger than the proportionality law and enable the additive mixture among post-transformed colors as well as for dichromats.

Keywords: dichromatic simulation, proportionality law, sRGB, video device gamut

1. Introduction

About 2.5% of male population are dichromats. Dichromats are color-blind persons missing one of the three cone systems in their eyes, and they cannot distinguish some colors that normal trichromats, persons having normal color vision, can distinguish. Such colors are called *confusion colors*.

Almost all dichromats are inherited and cannot change their color vision in their life. Thus, the color universal design to avoid danger and inconvenience caused by confusion colors are preferred. The most common tools used by designers are the computer simulation of images which transforms images into those that dichromats see.

Standard computer simulation algorithms of color appearance for dichromats were proposed by Brettel et al. in 1997 [1], [2]. Nowadays this algorithm is implemented in many computer applications, such as Vischeck [3] for image processing software and Chromatic Vision Simulator [4], [5] for smart phones, and is chosen as a reference data among several more elaborate dichromatic simulation algorithms [6]. We denote this algorithm as A97.

[1] Graduate School of Medical Sciences, Kitasato University, Sagamihara, Kanagawa 252–0373, Japan
[2] Graduate School of Medicine, The University of Tokyo, Bunkyo, Tokyo 113–0033, Japan
[3] University of Shizuoka, Shizuoka 222–8526, Japan
[a)] fukuda@kitasato-u.ac.jp
[b)] hara@bme.gr.jp
[c)] asaken@kitasato-u.ac.jp
[d)] hitoshi@kitasato-u.ac.jp
[e)] noshiromakoto@gmail.com
[f)] mitsuaki.katsuya.jurigi@gmail.com

It is well known that A97 cannot simulate all colors that video devices can support as the authors already indicated in their paper [1]. This is the reason why they proposed another algorithm in 1999 [7] which can simulate all colors on the device. We denote this algorithm as A99. The modification in A99, however, has defects as the simulated colors are not the confusion colors. In any dichromatic simulation the simulated color at least needs to be a confusion color. However, this defect may be practically unworthy of attention because this simulated color is very close to the confusion color in the standard sRGB video display [8]. Furthermore A99 is a display dependent algorithm and it works only for the sRGB video display. Thus A99 is not a satisfactory modification of A97.

In this work, rather than pursuing the simulation of color perception, we consider the simulation of color confusion for dichromats for all colors that video devices can support under some guiding principles. From a point of view of the computer algorithms, both simulations are about choosing a representative color $s(Q)$ among the set of confusion colors for a given color Q. In the simulation of color perception, the representative or the function of Q, $s(Q)$ is determined based on the reports on unilateral inherited color vision deficiencies [9], [10], [11] or the human color vision mechanism [6]. Instead, in our simulation of color confusion, we will determine $s(Q)$ by the demand that for any Q in the display color gamut G, $s(Q)$ exists in G as well under some reasonable guiding principles. Recent works [6], [12] on dichromatic simulations are not focused on display color gamut like A99 or the present work but on better algorithms of color perception from the viewpoint of human color vision mechanism.

In Section 2, after explaining A97 and A99 with the same stan-

dard device sRGB and in the same cone fundamentals, we make the relation between A97 and A99 clear, and show how numerically serious the problems are. In Section 3, we turn to a guiding principle in the simulation of color confusion, namely a proportionality law and propose a new algorithm for general devices including sRGB in Section 4. In Section 5, experimental results of responses from dichromats for A97, A99 and our new algorithm are shown. In Section 6, we discuss another guiding principle, namely additivity law. Section 7 is the summary and discussion.

2. Relation between the Brettel et al. 1997 and Viénot et al. 1999 Algorithms

In this paper, we use CIE 1931 XYZ color specification system and use LMS system derived from Smith and Pokorny [7], [8] for normal trichromats (normal people),

$$\begin{pmatrix} L \\ M \\ S \end{pmatrix} = \boldsymbol{U} \begin{pmatrix} X \\ Y \\ Z \end{pmatrix}, \tag{1}$$

where

$$\boldsymbol{U} = \begin{pmatrix} 0.15514 & 0.54312 & -0.03286 \\ -0.15514 & 0.45684 & 0.03286 \\ 0 & 0 & 0.01608 \end{pmatrix}. \tag{2}$$

L, M, and S specify colors in terms of the relative excitations of longwave sensitive, middlewave sensitive, and shortwave sensitive cones, respectively. It is assumed that the three kinds of dichromats, protanopes, deuteranopes and tritanopes, cannot perceive any change in L, M, and S, respectively. In other words, the confusion colors of a color stimulus $\boldsymbol{Q} = (L, M, S)^T$, where T denotes the matrix transpose, are on the line

$$l_a(\boldsymbol{Q}) = \{\boldsymbol{Q} + \hat{a}t | t = \text{real}\} \tag{3}$$

parallel to $a = L, M$ and S axis passing through $\boldsymbol{Q}$ in this LMS space, respectively. $\hat{a}$ in Eq. (3) represents the unit vector for $a = L, M$ and S axis.

In order to define a representative color $\boldsymbol{s}(\boldsymbol{Q})$ among the confusion colors $l_a(\boldsymbol{Q})$, the surface

$$\Sigma = \{ \begin{pmatrix} L \\ M \\ S \end{pmatrix} | u(L, M, S) = 0\} \tag{4}$$

is introduced, where $u(L, M, S)$ is a real function in the form

$$u(L, M, S) = \begin{cases} L - u_L(M, S) \text{ for protanopes,} \\ M - u_M(S, L) \text{ for deuteranopes,} \\ S - u_S(L, M) \text{ for tritanopes.} \end{cases} \tag{5}$$

Thus the color $\boldsymbol{s}(\boldsymbol{Q})$ is the crossing point between the surface Σ and the line $l_a(\boldsymbol{Q})$

$$\boldsymbol{s}(\boldsymbol{Q}) = \Sigma \cap l_a(\boldsymbol{Q}), \tag{6}$$

where $a = L, M$, or S for protanope, deuteranope, and tritanope, respectively. **Figure 1** shows this geometrical scheme among $\boldsymbol{Q}$, $l_L(\boldsymbol{Q})$, Σ and $\boldsymbol{s}(\boldsymbol{Q})$ for protanopes. In Fig. 1, the bended surface is Σ which is used in A97 explained in the next section.

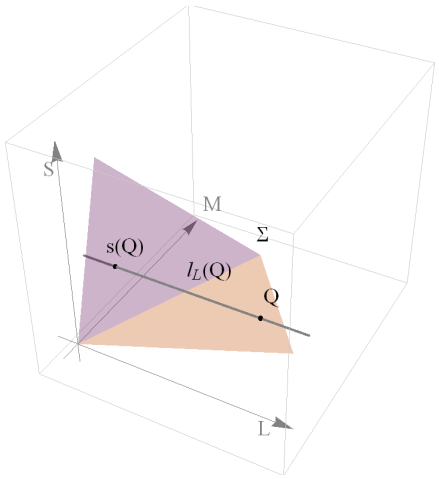

Fig. 1 Geometrical scheme to determine $\boldsymbol{s}(\boldsymbol{Q})$ from $\boldsymbol{Q}$ as crossing point between $l_L(\boldsymbol{Q})$ and Σ for protanopes in LMS space. The bended surface is Σ which is used in A97.

We call $\boldsymbol{s}(\boldsymbol{Q})$ as *simulation function* and Σ as *simulation surface*, respectively, and define *simulation of color confusion*.

Simulation of color confusion. *Input: a picture I composed of $w \times h$ pixels whose color at (i, j) position is $\boldsymbol{Q}_{ij}$. Output: a picture $s(I)$ composed of $w \times h$ pixels whose color at (i, j) position is $\boldsymbol{s}(\boldsymbol{Q}_{ij})$.*

Note that there is no more restriction on simulation function $\boldsymbol{s}(\boldsymbol{Q})$ and accordingly on simulation surface Σ. Thus, in the simulation of color confusion, simulation surface Σ can be either piecewise planar as shown in Fig. 1 or non-planar (curved) surface used in [6].

2.1 A97: Brettel et al. 1997 Algorithms

In accordance with the reports on unilateral inherited color vision deficiencies [9], [10], [11], which stated that all colors were seen as colors with dominant wavelength either λ_1 or λ_2, A97 defined the simulation surface Σ as

$$\Sigma(\lambda_1, \lambda_2) = \Sigma(\lambda_1) \cup \Sigma(\lambda_2), \tag{7}$$

$$\Sigma(\lambda_i) = \{\alpha \boldsymbol{E} + \beta \boldsymbol{C}(\lambda_i) | \alpha \geq 0, \beta \geq 0\}, i = 1, 2, \tag{8}$$

where $\boldsymbol{E} = \boldsymbol{U}(1, 1, 1)^T$ is equal-energy stimulus and

$$\boldsymbol{C}(\lambda) = \boldsymbol{U} \begin{pmatrix} \bar{x}(\lambda) \\ \bar{y}(\lambda) \\ \bar{z}(\lambda) \end{pmatrix} \tag{9}$$

is monochromatic stimulus. Here $\bar{x}(\lambda)$, $\bar{y}(\lambda)$ and $\bar{z}(\lambda)$ are the CIE 1931 standard color matching functions. $\Sigma(\lambda_i)$ in Eq. (8) is a planar region bounded by two half-line from origin parallel to $\boldsymbol{E}$ and $\boldsymbol{C}(\lambda_i)$. For protanopes and deuteranopes $\lambda_1 = 475$ nm and $\lambda_2 = 575$ nm are adopted, and for tritanopes, $\lambda_1 = 485$ nm and $\lambda_2 = 660$ nm. The simulation surface Σ shown in Fig. 1 is actually $\Sigma(475, 575)$.

In these cases, the simulation surface is called *stimulus surface* because it is a common color stimulus perceived by both dichromats and normal trichromatic observers. In general,

Simulation of color perception. *The simulation of color confu-*

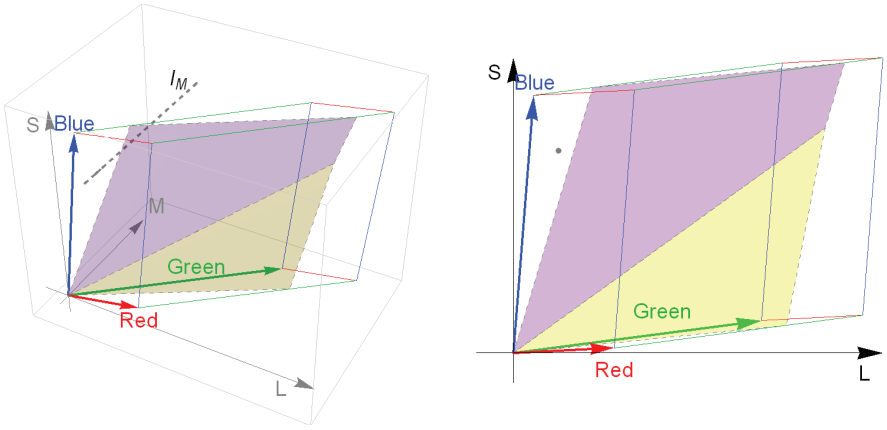

Fig. 2 Intersection of the stimulus surface $\Sigma(475, 575)$ of A97 and the sRGB-parallelepiped. If we look at the left figure from the M axis, we obtain the right figure. Dashed line l_M in the left figure, a line parallel to M-axis, is passing through the sRGB-parallelepiped but does not intersect with $\Sigma(475, 575)$ in the sRGB-parallelepiped. A point near S-axis in the right figure is the l_M.

sion $s(I)$ of a picture I is called the simulation of color perception $s^*(I)$ if stimulus surface is used as the simulation surface.

If a unilateral subject looks at the simulation of color perception $s^*(I)$ with his normal trichromatic eye and at the original picture I with his dichromatic eye, he cannot find any differences between two pictures. However, if he looks at the simulation of color confusion $s(I)$ instead of $s^*(I)$ he will find differences. Of course, dichromats whose eyes are both dichromatic cannot distinguish three pictures I, $s(I)$ and $s^*(I)$.

Now we introduce sRGB video devices as the most popular type of displays. The sRGB color stimuli are represented by 8-bit DAC values (r, g, b) for $r, g, b = 0, 1, 2, \ldots, 255$ and these stimuli are included in the parallelepiped defined by Red=$(255, 0, 0)$, Green=$(0, 255, 0)$ and Blue=$(0, 0, 255)$ primaries in sRGB. We call this parallelepiped the sRGB-parallelepiped.

In **Fig. 2** (left), the intersection of the stimulus surface $\Sigma(475, 575)$ shown in Fig. 1 and the sRGB-parallelepiped is shown. If we look at the Fig. 2 (left) from the M axis, we obtain the Fig. 2 (right). We can see from the Fig. 2 (right) for some stimulus $\boldsymbol{Q}$ in the sRGB-parallelepiped, the line $l_M(\boldsymbol{Q})$ does not cross the stimulus surface $\Sigma(475, 575)$ in the sRGB-parallelepiped, that is, the intersection of the stimulus surface $\Sigma(475, 575)$ and the sRGB-parallelepiped. The dashed line labeled l_M in Fig. 2 (left) is an example of such $l_M(\boldsymbol{Q})$. The l_M has points in the sRGB-parallelepiped, $\boldsymbol{Q}$, but does not intersect with $\Sigma(475, 575)$ in the sRGB-parallelepiped. A point near S-axis in Fig. 2 (right) is the l_M. This means that the stimulus surface $\Sigma(475, 575)$ cannot be adopted to simulate all $256^3 = 16777216$ colors for deuteranopes. This problem also exists for protanope and tritanope simulations.

In **Table 1**, we present the number of sRGB colors (r, g, b) which cannot be simulated by A97. We consider those numbers as rather large to neglect. Note that irrespective of the devices some colors cannot be simulated by A97 as shown in Fig. 6 of Ref. [6]. To our knowledge, it is not known whether the dichromatic eye and normal trichromatic eye of unilateral dichromats can match these colors or not.

Table 1 Number of sRGB colors which cannot be simulated by A97. In the column labeled N the numbers of colors which cannot be simulated by A97 are tabulated, and in "Ratio" the ratios between N and the total number of sRGB colors (256^3).

Type of simulation	N	Ratio
Protanopes	4,669,975	27.8%
Deuteranopes	2,621,467	15.6%
Tritanopes	2,797,874	16.7%

Table 2 Number of sRGB colors which cannot be simulated by A99 without color domain transformation (11). In the column labeled N the numbers of colors which cannot be simulated by A99 without domain transformation (11) are tabulated, and in "Ratio" the ratios between N and the total number of sRGB colors (256^3).

Type of simulation	N	Ratio
Protanopes	190,447	1.1%
Deuteranopes	634,406	3.8%

2.2 A99: Viénot et al. 1999 Algorithms

For sRGB video devices, in A99, $\boldsymbol{E}$, $\boldsymbol{C}(475)$, and $\boldsymbol{C}(575)$ which determine $\Sigma(475, 575)$ in A97 are approximated by colors of 8-bit sRGB value $\boldsymbol{Uf}(255, 255, 255)$, $\boldsymbol{Uf}(0, 0, 255)$ and $\boldsymbol{Uf}(255, 255, 0)$, respectively, where $\boldsymbol{f}(r, g, b)$ is the column vector function which transforms (r, g, b) to $(X, Y, Z)^T$ according to the formula in Ref. [8]. Since $\boldsymbol{f}(255, 255, 255) = \boldsymbol{f}(0, 0, 255) + \boldsymbol{f}(255, 255, 0)$, two planar parts $\Sigma(475)$ and $\Sigma(575)$ in $\Sigma(475, 575)$ become parallel in A99 and stimulus surface for protanopes and deuteranopes is the plane

$$\Sigma^{(99)} = \{\alpha \boldsymbol{Uf}(0, 0, 255) + \beta \boldsymbol{Uf}(255, 255, 0) | \alpha \text{ and } \beta \text{ are real}\}. \tag{10}$$

A tritanope simulation and video devices other than sRGB are not supported in A99.

Again, not all lines $l_L(\boldsymbol{Q})$ or $l_M(\boldsymbol{Q})$ for $\boldsymbol{Q} = \boldsymbol{Uf}(r, g, b)$ cross the stimuli surface $\Sigma^{(99)}$ in the sRGB-parallelepiped. Thus there also exists the same problem in the $\Sigma^{(99)}$ as in A97. In **Table 2**, we show the number of sRGB colors which cannot be simulated by $\Sigma^{(99)}$.

Since these numbers are small, A99 introduced the following color domain transformation

$$\boldsymbol{f}^*(r, g, b) = c_1 \boldsymbol{f}(r, g, b) + c_2 \boldsymbol{f}(255, 255, 255) \tag{11}$$

where $c_1 = 1.0092$ and $c_2 = -0.0046$ for protanopes, and $c_1 = 0.9420$ and $c_2 = 0.0264$ for deuteranopes. These coefficients are slightly different from those in Ref. [7], since in Ref. [7] a different LMS space is adopted. For the modified stimulus $\boldsymbol{Q}^* = \boldsymbol{Uf}^*(r,g,b)$ all lines $l_L(\boldsymbol{Q}^*)$ or $l_M(\boldsymbol{Q}^*)$ cross the stimulus surface $\Sigma^{(99)}$ in the sRGB-parallelepiped. Namely in A99 after color domain transformation (11) all colors of sRGB can be simulated.

We should notice that although the transformation (11) is almost identical, the simulated color $\boldsymbol{s}(\boldsymbol{Q}^*)$ is not the confusion color of $\boldsymbol{Q}$ but the confusion color of $\boldsymbol{Q}^*$. This means dichromats may perceive the difference between $\boldsymbol{Q}$ and $\boldsymbol{Q}^*$; therefore, strictly speaking, A99 with this transformation is not a dichromatic simulation.

Note that the transformation of a unit or scale in L, M, or S does not affect the above mentioned problem either for A97 or $\Sigma^{(99)}$, that is, Table 1 and Table 2 are unchanged.

3. Proportionality Law

The stimulus surface $\Sigma(\lambda_1, \lambda_2)$ of A97 has a special shape, called cone. If a point is on the stimulus surface $\Sigma(\lambda_1, \lambda_2)$, the line segment connecting the point and the origin is always included in the same surface $\Sigma(\lambda_1, \lambda_2)$. This means in the simulation surface with cone shape, if a color stimulus $\boldsymbol{Q}$ is simulated by $\boldsymbol{s}(\boldsymbol{Q})$ then color stimulus $\alpha\boldsymbol{Q}$ proportional to $\boldsymbol{Q}$ is simulated by $\alpha\boldsymbol{s}(\boldsymbol{Q})$. Thus A97 implies that the proportionality law, $\boldsymbol{s}(\alpha\boldsymbol{Q}) = \alpha\boldsymbol{s}(\boldsymbol{Q})$, between the dichromatic eye and normal trichromatic eye holds although the authors of A97 did not refer to this law explicitly. We simply call this law the proportionality law.

Proportionality law. *If color stimulus $\boldsymbol{Q}$ is simulated by $\boldsymbol{s}(\boldsymbol{Q})$, then proportional color stimulus $\alpha\boldsymbol{Q}$ is simulated by $\alpha\boldsymbol{s}(\boldsymbol{Q})$, that is, $\boldsymbol{s}(\alpha\boldsymbol{Q}) = \alpha\boldsymbol{s}(\boldsymbol{Q})$ holds.*

Inversely we can state that if the simulations do not contradict with this proportionality law, their stimuli surfaces must be a cone with its apex at the origin.

For normal trichromats, the vector $\alpha\boldsymbol{Q}$ proportional to $\boldsymbol{Q}$ represents the same color with different intensity, and vectors with different direction do not represent the same color. Thus, if the proportionality law holds, the same color $\alpha\boldsymbol{Q}$ with different intensity are simulated by one color $\alpha\boldsymbol{s}(\boldsymbol{Q})$, and vice versa. Without the proportionality law, the same color $\alpha\boldsymbol{Q}$ with different intensity will be simulated by several different colors.

Since this seems to be a fundamental requirement in dichromatic simulation in early-stage, we will discuss a simulation function $\boldsymbol{s}(\boldsymbol{Q})$ which can support all colors on a device while satisfying this proportionality law.

4. Simulation Function $s(Q)$ in a Device Gamut with the Proportionality Law

We discuss the general device described by an ICC profile with device color primaries $\boldsymbol{E}_1$, $\boldsymbol{E}_2$ and $\boldsymbol{E}_3$ in a LMS space as defined in Section 2. For sRGB these are

$$\begin{aligned}
\boldsymbol{E}_1 &= \text{Red} = \boldsymbol{Uf}(255,0,0),\\
\boldsymbol{E}_2 &= \text{Green} = \boldsymbol{Uf}(0,255,0),\\
\boldsymbol{E}_3 &= \text{Blue} = \boldsymbol{Uf}(0,0,255).
\end{aligned} \tag{12}$$

We will show that for a given set of $\boldsymbol{E}_1$, $\boldsymbol{E}_2$ and $\boldsymbol{E}_3$, the simulation function $\boldsymbol{s}(\boldsymbol{Q})$ which can support all colors on the device gamut while satisfying the proportionality law is uniquely determined except for two rare cases. In general, if we look at three primary vectors $\boldsymbol{E}_1, \boldsymbol{E}_2, \boldsymbol{E}_3$ from one of axes $a = L$, M or S, we will see three non-zero vectors, for instance those labeled "Red," "Green" and "Blue" in Fig. 2 (right) for sRGB, which are projected vectors of $\boldsymbol{E}_1, \boldsymbol{E}_2, \boldsymbol{E}_3$ into the plane perpendicular to the axis $a = M$. We will consider this case in the following and exceptional cases where we cannot see three projected vectors will be considered in Appendix A.1 for completeness' sake.

We define projection operator

$$\boldsymbol{P} = \begin{pmatrix} 0 & 1 & 0 \\ 0 & 0 & 1 \end{pmatrix}, \text{or} \begin{pmatrix} 1 & 0 & 0 \\ 0 & 0 & 1 \end{pmatrix}, \text{or} \begin{pmatrix} 1 & 0 & 0 \\ 0 & 1 & 0 \end{pmatrix} \tag{13}$$

for protanopes, deuteranopes and tritanopes, respectively. Then, we consider three projected vectors in two dimensions, $\boldsymbol{PE}_k, k = 1,2,3$. We rename vectors $\boldsymbol{E}_k$ using descending order of the first component of the normalized projected vectors $\hat{V}_k$, defined by $\hat{V}_k = \boldsymbol{PE}_k/|\boldsymbol{PE}_k|$ for $\boldsymbol{PE}_k \neq \boldsymbol{0}$ and $\hat{V}_k = \boldsymbol{0}$ for $\boldsymbol{PE}_k = \boldsymbol{0}$.

Theorem 1. *When $\hat{V}_1 \neq \boldsymbol{0}$, $\hat{V}_2 \neq \boldsymbol{0}$, $\hat{V}_3 \neq \boldsymbol{0}$ and $\hat{V}_1 \neq \hat{V}_2 \neq \hat{V}_3 \neq \hat{V}_1$, the simulation function $\boldsymbol{s}(\boldsymbol{Q})$ with the following properties (P1) and (P2) are unique. (P1) For all $\boldsymbol{Q}$ in the parallelepiped $\boldsymbol{E}_1\boldsymbol{E}_2\boldsymbol{E}_3$ $\boldsymbol{s}(\boldsymbol{Q})$ is also in the parallelepiped $\boldsymbol{E}_1\boldsymbol{E}_2\boldsymbol{E}_3$. (P2) $\boldsymbol{s}(\boldsymbol{Q})$ satisfies the proportionality law, $\boldsymbol{s}(\alpha\boldsymbol{Q}) = \alpha\boldsymbol{s}(\boldsymbol{Q})$. The simulation surface which define the $\boldsymbol{s}(\boldsymbol{Q})$ is*

$$\begin{aligned}
\Sigma^{(g)} &= \Sigma_1 \cup \Sigma_2 \cup \Sigma_3 \cup \Sigma_4,\\
\Sigma_1 &= \{p\boldsymbol{E}_1 + q(\boldsymbol{E}_1 + \boldsymbol{E}_2) | p,q \geq 0, p+q \leq 1\},\\
\Sigma_2 &= \{p(\boldsymbol{E}_1 + \boldsymbol{E}_2) + q(\boldsymbol{E}_1 + \boldsymbol{E}_2 + \boldsymbol{E}_3) | p,q \geq 0, p+q \leq 1\},\\
\Sigma_3 &= \{p(\boldsymbol{E}_1 + \boldsymbol{E}_2 + \boldsymbol{E}_3) + q(\boldsymbol{E}_2 + \boldsymbol{E}_3) | p,q \geq 0, p+q \leq 1\},\\
\Sigma_4 &= \{p(\boldsymbol{E}_2 + \boldsymbol{E}_3) + q\boldsymbol{E}_3 | p,q \geq 0, p+q \leq 1\}.
\end{aligned} \tag{14}$$

Proof: The parallelepiped $\boldsymbol{E}_1\boldsymbol{E}_2\boldsymbol{E}_3$ spanned by $\boldsymbol{E}_1, \boldsymbol{E}_2$ and $\boldsymbol{E}_3$ is projected by $\boldsymbol{P}$ to a hexagon and the edges of the hexagon are the projections of the following six edges of the parallelepiped $\boldsymbol{E}_1\boldsymbol{E}_2\boldsymbol{E}_3$

$$\begin{aligned}
e_1 &= \{t\boldsymbol{E}_1 | 0 \leq t \leq 1\},\\
e_2 &= \{t\boldsymbol{E}_1 + (1-t)(\boldsymbol{E}_1 + \boldsymbol{E}_2) | 0 \leq t \leq 1\},\\
e_3 &= \{t(\boldsymbol{E}_1 + \boldsymbol{E}_2) + (1-t)(\boldsymbol{E}_1 + \boldsymbol{E}_2 + \boldsymbol{E}_3) | 0 \leq t \leq 1\},\\
e_4 &= \{t(\boldsymbol{E}_1 + \boldsymbol{E}_2 + \boldsymbol{E}_3) + (1-t)(\boldsymbol{E}_2 + \boldsymbol{E}_3) | 0 \leq t \leq 1\},\\
e_5 &= \{t(\boldsymbol{E}_2 + \boldsymbol{E}_2) + (1-t)\boldsymbol{E}_3 | 0 \leq t \leq 1\},\\
e_6 &= \{t\boldsymbol{E}_3 | 0 \leq t \leq 1\}.
\end{aligned} \tag{15}$$

Figure 2 (right) is an example of sRGB for deuteranopes. The projected vectors $\boldsymbol{PE}_1, \boldsymbol{PE}_2$ and $\boldsymbol{PE}_3$ are the vectors denoted by "Blue," "Green" and "Red," respectively, and the e_i, $i = 1,2,\ldots,6$ are the edges in the hexagonal envelope (outer most

hexagon) of the sRGB-parallelepiped.

Since $\boldsymbol{Q}$ on e_i in the parallelepiped $\boldsymbol{E}_1\boldsymbol{E}_2\boldsymbol{E}_3$ has no common point with the $l_a(\boldsymbol{Q})$ except for $\boldsymbol{Q}$ itself, all edges e_i, $i = 1, 2, \ldots, 6$, must be included in the simulation surface Σ which defines $\boldsymbol{s}(\boldsymbol{Q})$ in order for $\boldsymbol{s}(\boldsymbol{Q})$ to be in the parallelepiped $\boldsymbol{E}_1\boldsymbol{E}_2\boldsymbol{E}_3$ as well. On the other hand, the proportionality law requires that the line segment connecting the origin and any point in e_i also be included in the simulation surface Σ. This determines the simulation surface Σ uniquely as Eq. (14). See **Fig. 3**. Q.E.D.

We illustrate the simulation surface (14) in **Fig. 4** by using the data of sRGB video device in LMS space defined in Section 2. The left figure is the surface $\Sigma^{(g)}$ for protanopes and tritanopes, and the right one for deuteranopes. They are different since for deuteranopes the primary vectors $\boldsymbol{E}_1, \boldsymbol{E}_2$ and $\boldsymbol{E}_3$ are the sRGB primaries "Blue," "Green" and "Red," respectively, as shown in Fig. 2 (right), while for protanopes and tritanopes those are "Blue," "Red" and "Green," respectively ("Green" and "Red" are interchanged).

We can see that the stimulus surface of A97 for protanopes and deuteranopes shown in Fig. 2 (left) are very different from the simulation surface $\Sigma^{(g)}$ shown in Fig. 4 (left) for protanopes and in Fig. 4 (right) for deuteranopes. If we look at these simulation surfaces from the L axis and M axis, respectively, we will not find any gaps such as we see in Fig. 2 (right) for A97. Accordingly ratios shown in Table 1 for A97 become 0%'s for $\Sigma^{(g)}$ as we intended.

The condition $\hat{V}_1 \neq \mathbf{0}$, $\hat{V}_2 \neq \mathbf{0}$, $\hat{V}_3 \neq \mathbf{0}$, $\hat{V}_1 \neq \hat{V}_2 \neq \hat{V}_3 \neq \hat{V}_1$ in theorem 1 is identical with the geometrical statement that the projection of the device gamut onto the plane perpendicular to the color confusion axis in LMS space is hexagon. The majority of devices including sRGB are this type and for these devices $\Sigma^{(g)}$ in Eq. (14) is the only possible surface defining $\boldsymbol{s}(\boldsymbol{Q})$ for all colors on the device while satisfying the proportionality law. We call our algorithm by theorem 1 as APL (algorithm based on proportionality law).

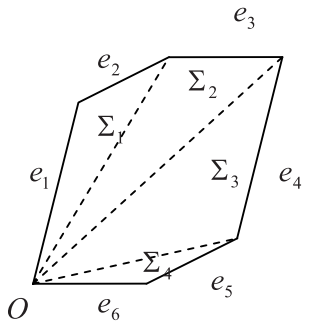

Fig. 3 Origin and six edges e_i, $i = 1, 2, \ldots, 6$ and four planar pieces Σ_i, $i = 1, 2, \ldots, 4$ of the simulation surface $\Sigma^{(g)}$.

5. Comparison of the Three Algorithms

We tested if the algorithms A97, A99, and our APL worked in the sense that the dichromatic observer could not find any differences between the original pictures and the transformed ones. **Figure 5** presents the original picture which is similar to the picture used in Ref. [1] and consists of 25 color cells selected randomly from sRGB 256^3 colors. The sRGB 8-bit (r, g, b) values of these 25 colors are listed in **Table 3**.

As a typical sRGB video display we used Mitsubishi LCD (Liquid Crystal Display), Dyamondcrysta RDT231WLM. The accuracy of this display is $\Delta = 0.064$ several hours after the power is on, where

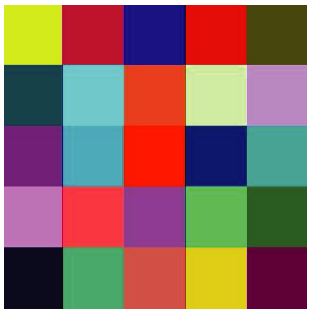

Fig. 5 The original picture (25 colored cells).

Table 3 sRGB 8-bit (r, g, b) values corresponding to the color cells in Fig. 5.

(222, 244, 69)	(191, 56, 78)	(33, 27, 174)	(222, 47, 47)	(95, 96, 5)
(14, 97, 103)	(38, 223, 240)	(227, 100, 70)	(205, 248, 189)	(200, 149, 238)
(133, 72, 133)	(37, 175, 207)	(252, 57, 6)	(32, 64, 133)	(46, 171, 174)
(211, 131, 223)	(250, 92, 93)	(154, 95, 155)	(12, 232, 135)	(54, 119, 69)
(4, 7, 55)	(55, 179, 139)	(209, 114, 99)	(227, 205, 73)	(116, 28, 79)

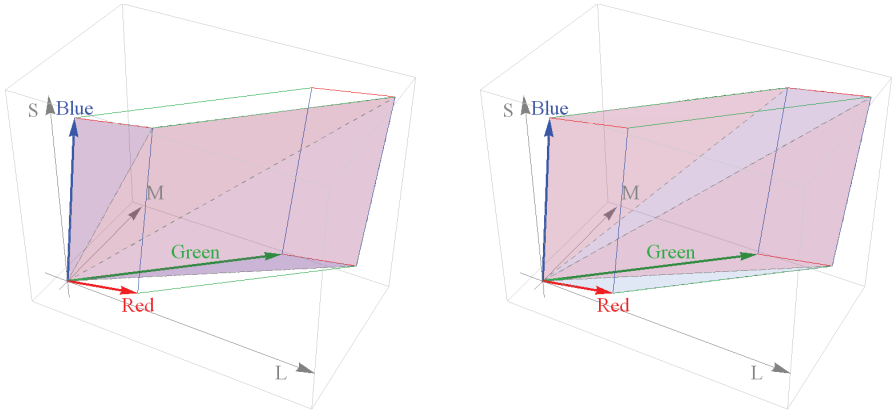

Fig. 4 Surface $\Sigma^{(g)}$ for protanopes and tritanope (left), and for deuteranope (right) in sRGB. In the left figure, the primary vectors $\boldsymbol{E}_1, \boldsymbol{E}_2$ and $\boldsymbol{E}_3$ are the vectors denoted by "Blue," "Red" and "Green," respectively, while in the right figure, those are "Blue," "Green" and "Red," respectively ("Green" and "Red" are interchanged).

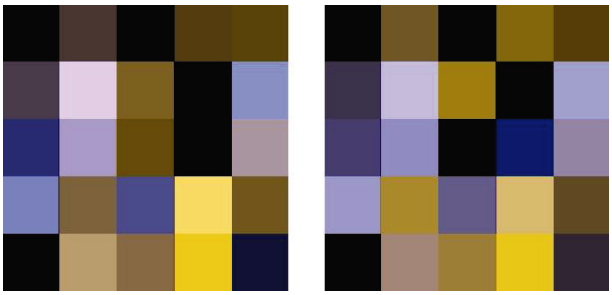

Fig. 6 Protanopic (left) and Deuteranopic (right) simulations of the original picture by A97. The colors which cannot be simulated by A97 are indicated by black. There are five black cells in protanopic and deuteranopic simulations.

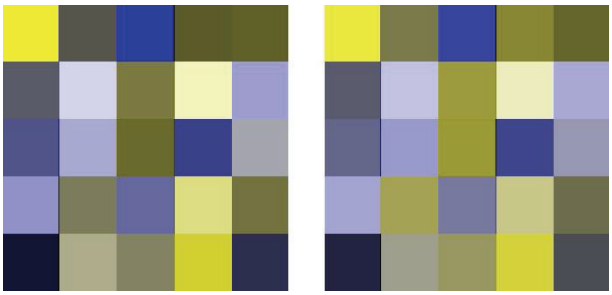

Fig. 7 Protanopic (left) and Deuteranopic (right) simulations of the original picture by A99.

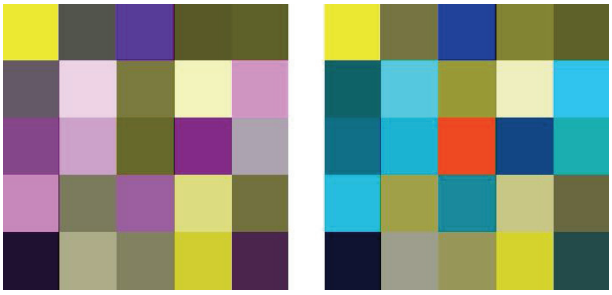

Fig. 8 Pictures by APL for Protanopic (left) and Deuteranopic (right).

$$\Delta = \sqrt{\frac{1}{n}\sum_i (\boldsymbol{f}(r_i, g_i, b_i) - (X_i, Y_i, Z_i)^T)^2}$$

for these $n = 25$ colors. (r_i, g_i, b_i) is the sRGB 8-bit value and $(X_i, Y_i, Z_i)^T$ is the corresponding measured value by a color analyzer (Display Color Analyzer CA-210, Konica Minolta, Inc) normalized as $Y = 1$ at $(255, 255, 255)$ sRGB 8-bit value.

Figure 6 illustrates the simulation result by A97, where five cells with black in protanopic and deuteranopic simulations show the colors which cannot be simulated by A97. These ratios of the number of the cells with black, $5/25 = 20\%$ for both simulations, do not statistically contradict with the ratios 27.8% and 15.6% tabulated in Table 1, respectively.

On the other hand, for A99, we used color domain transformation (11) and thus all 25 colors are simulated as shown in **Fig. 7** though all of them are not confusion colors.

For our APL all 25 colors are displayed as shown in **Fig. 8** since APL can support all colors for any video devices. As we explained in Section 2, Fig. 6 is the most reliable dichromatic simulation and Fig. 7 is its approximation, and thus they are similar. However, Fig. 8 is quite different from Fig. 6 (or Fig. 7) because Fig. 8 is not the result of the simulation of color perception but of color confusion using the simulation surfaces shown in Fig. 4 which have completely different shapes from the well-known stimulus surface of A97 shown in Fig. 2 (left).

We studied whether three dichromatic observers, one protanope and two deuteranopes, could distinguish color cells in original pictures from those by A97, A99 and APL or not.

The tasks of the experiment are as follows:

(1) In a darkroom, we show two pictures in the display, the original picture Fig. 5 on the left hand side, and the simulated picture which is one of pictures shown in Fig. 6–Fig. 8 or tritanopic results by A97 and APL on the right hand side.
(2) We point one of 25 cells in the original picture by mouse pointer in raster scan order, and ask a test subject whether the color in the cell is similar to the corresponding cell on the right hand side.
(3) We change the picture on the right hand side after 25 questions and continue to ask the next 25 questions.
(4) The picture on the right hand side is changed 20 times in the following order:

    (1-A97-P/D), (1-APL-P/D),
    A97-P, A97-D, A97-T, APL-P, APL-D, APL-T, A99-P, A99-D,
    (2-A97-P/D), (2-APL-P/D),
    A97-P, A97-D, A97-T, APL-P, APL-D, APL-T, A99-P, A99-D,

    The label in the form X-Y-Z or Y-Z indicates the picture. No X means the picture in Fig. 5 and different X's the other original pictures. Y is the method, and Z the type of dichromats. P/D corresponds to the type of the test subject P or D. Two series of 8 succeeding terms beginning from the third and 13th term are the same.
(5) The 4 results in the parentheses are discarded, and we have checked that the two series of 8 results coincide.

After this experiment, we gained the results that they found no difference between original and the transformed pictures adjusted to their dichromatic types, and when protanopic (deuteranopic) patients looked at the pictures for the deuteranopic (protanopic) results they found some differences. Although our test subjects are only three without tritanopes, we conclude that all three methods, A97, A99 and APL work as simulation of color confusion because they are based on a well-established model for color confusion. For A99, though it uses approximate confusion colors, all test subjects could not detect this approximation in this experiment.

We note that the APL is the algorithm for any display devices in which sRGB display is not necessarily assumed. In this section we have shown the APL woks on sRGB as a sample of display devices. Therefore we assure that APL can work on any other display devices.

6. Additivity Law

The stimulus surface $\Sigma(475, 575)$ of A97 for protanopes and deuteranopes shown in Fig. 2 (left) is almost like a plane, that is, two parts $\Sigma(475)$ and $\Sigma(575)$ are almost parallel. If they are exactly parallel the following additivity law also holds for dichro-

matic simulation like the proportionality law.

Additivity law. *If color stimuli $\boldsymbol{Q}_1$ and $\boldsymbol{Q}_2$ are simulated by $\boldsymbol{s}(\boldsymbol{Q}_1)$ and $\boldsymbol{s}(\boldsymbol{Q}_2)$, respectively, then an additivity color stimulus $\boldsymbol{Q}_1 + \boldsymbol{Q}_2$ is simulated by $\boldsymbol{s}(\boldsymbol{Q}_1) + \boldsymbol{s}(\boldsymbol{Q}_2)$, that is, $\boldsymbol{s}(\boldsymbol{Q}_1 + \boldsymbol{Q}_2) = \boldsymbol{s}(\boldsymbol{Q}_1) + \boldsymbol{s}(\boldsymbol{Q}_2)$ holds.*

For both normal trichromats and dichromats, an addition of two vectors, $\boldsymbol{Q}_1 + \boldsymbol{Q}_2$ is the additive mixture of the two colors $\boldsymbol{Q}_1$ and $\boldsymbol{Q}_2$. Therefore, for simulated colors it is preferable that an addition $\boldsymbol{s}(\boldsymbol{Q}_1) + \boldsymbol{s}(\boldsymbol{Q}_2)$ is also a simulated color. Since the additivity law ensures this property, we are interested in the additivity law.

The inverse statement that if the additivity law holds the simulation surface must be a plane which includes the origin, is easily verified because the proportionality law always holds when the additivity law holds. Mathematically if a continuous function $\boldsymbol{s}(\boldsymbol{Q})$ of vector $\boldsymbol{Q}$ with real component is additive, i.e., $\boldsymbol{s}(\boldsymbol{Q}_1 + \boldsymbol{Q}_2) = \boldsymbol{s}(\boldsymbol{Q}_1) + \boldsymbol{s}(\boldsymbol{Q}_2)$, then $\boldsymbol{s}(\boldsymbol{Q})$ is proportional, i.e., $\boldsymbol{s}(\alpha\boldsymbol{Q}) = \alpha\boldsymbol{s}(\boldsymbol{Q})$. Therefore we will obtain following corollary 1 from the theorem 1 for the majority of the devices. Exceptional cases where we cannot see three projected vectors will be considered in corollaries in Appendix A.1 for the sake of completeness.

Corollary 1. *In the notation of theorem 1, when $\hat{V}_1 \neq 0$, $\hat{V}_2 \neq 0$, $\hat{V}_3 \neq 0$ and $\hat{V}_1 \neq \hat{V}_2 \neq \hat{V}_3 \neq \hat{V}_1$, the simulation function $\boldsymbol{s}(\boldsymbol{Q})$ having both properties (P1) in theorem 1 and (P3) in the following does not exist. (P3) $\boldsymbol{s}(\boldsymbol{Q})$ satisfies the additivity law, $\boldsymbol{s}(\boldsymbol{Q}_1 + \boldsymbol{Q}_2) = \boldsymbol{s}(\boldsymbol{Q}_1) + \boldsymbol{s}(\boldsymbol{Q}_2)$.*

Proof: Suppose $\boldsymbol{s}(\boldsymbol{Q})$ satisfies both (P1) and (P3) then $\boldsymbol{s}(\boldsymbol{Q})$ satisfies proportionality law as stated above. Thus by theorem 1, $\boldsymbol{s}(\boldsymbol{Q})$ is unique and defined by the surface $\Sigma^{(g)}$ in Eq. (14).

We investigate Σ_1 and Σ_2 in (14) which constitute $\Sigma^{(g)}$. Σ_1 is on the plane S_1 spanned by $\boldsymbol{E}_1$ and $\boldsymbol{E}_1 + \boldsymbol{E}_2$, and Σ_2 is on the plane S_2 spanned by $\boldsymbol{E}_1 + \boldsymbol{E}_2$ and $\boldsymbol{E}_1 + \boldsymbol{E}_2 + \boldsymbol{E}_3$. Since $\boldsymbol{E}_1$, $\boldsymbol{E}_2$ and $\boldsymbol{E}_3$ are independent, after some vector algebra, we can show that $S_1 \cap S_2$ is a line passing through the origin directed to the vector $\boldsymbol{E}_1 + \boldsymbol{E}_2$. This means S_1 and S_2 are not parallel and accordingly Σ_1 and Σ_2 are not. Therefore the surface Eq. (14) is not a plane. This contradicts that $\boldsymbol{s}(\boldsymbol{Q})$ satisfies the additivity law. Q.E.D.

7. Summary and Discussions

We have assumed a standard model of confusion color for dichromatic observer, which is composed of the LMS space such as Eqs. (1) and (2), and the set of confusion colors in Eq. (3). Within this model, we have shown our main result that a dichromatic simulation function $\boldsymbol{s}(\boldsymbol{Q})$ for any color $\boldsymbol{Q}$ in display color gamut G, is uniquely determined if we demand the proportionality law, $\boldsymbol{s}(\alpha\boldsymbol{Q}) = \alpha\boldsymbol{s}(\boldsymbol{Q})$, for devices whose projected gamut G onto the plane perpendicular to the color confusion axis is hexagon in LMS space. The $\boldsymbol{s}(\boldsymbol{Q})$ is given by the intersection between the unique simulation surface $\Sigma^{(g)}$ and the line $l_a(\boldsymbol{Q})$ in Eq. (3). For devices with $n = 3$ video device primaries such as sRGB video devices in Eq. (12), the unique simulation surface $\Sigma^{(g)}$ is given by Eq. (14).

In **Fig. 9**, examples for simulation results on a real image, a photograph of Kitasato University, created by the three methods A97, A99 and APL for protanopes (P), deuteranopes (D) and tritanopes (T) are shown. We note the followings.

(1) Black pixel corresponding to non-black pixel in the original image shows that the pixel cannot be simulated. We call this pixel skipped pixel below.
(2) Skipped pixels exist only in the results by A97; however, A97 is the most reliable simulation of color perception.
(3) The results of A99 are similar to those of A97, and those of A99 have no skipped pixel. A99, however, does not satisfy

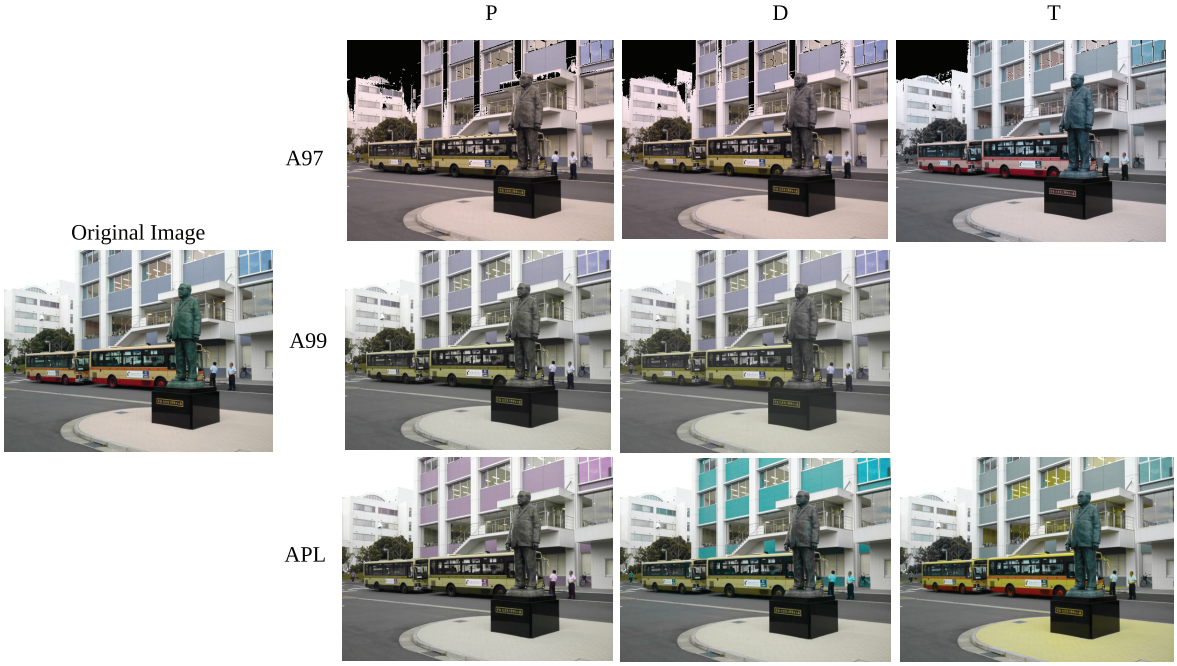

Fig. 9 Simulation results for protanopes (P), deuteranopes (D) and tritanopes (T) of a photograph of Kitasato University by the three methods A97, A99 and APL.

the fundamental requirement that simulated colors have to be confusion colors within the standard model.

(4) The results of APL are not similar to those by A97, since APL is not the simulation of color perception but the simulation of color confusion. However, APL has no skipped pixel and satisfy the proportionality law.

For devices with $n \geq 4$ video device primaries such as "Quattron" developed by Sharp Corporation, the parallelepiped of display gamut G and its projected hexagon in Fig. 3 will be zonohedron and convex polygon, respectively. In general, any edge of the convex polygon which is a projection of the zonohedron by $\boldsymbol{P}$ in Eq. (13) corresponds to an edge of zonohedron (not more than two edges). In this "general case" for $n \geq 4$, the projected convex polygon corresponding to Fig. 3 will have $2n$ vertices

$$\boldsymbol{v}_i = \sum_{j=1}^{i} \boldsymbol{PE}_j,\ \boldsymbol{v}_{n+i} = \sum_{j=1}^{i} \boldsymbol{PE}_{n-j-1},\ i = 1, 2, \ldots, n,$$

and $2n$ edges

$$\boldsymbol{e}_i = \boldsymbol{v}_{i+1} - \boldsymbol{v}_i,\ (\boldsymbol{v}_{2n+1} = \boldsymbol{v}_1),\ i = 1, 2, \ldots, 2n,$$

with $\boldsymbol{e}_j \parallel \boldsymbol{e}_{n+j} \parallel \boldsymbol{PE}_j$, $j = 1, 2, \ldots, n$. We will obtain the $2n - 2$ planar parts Σ_i from this figure as in Fig. 3 and then the unique simulation surface

$$\Sigma^{(g)} = \Sigma_1 \cup \Sigma_2 \cup \cdots \cup \Sigma_{2n-2}.$$

As a corollary of our main results, we have shown that it is impossible to build the algorithm for such devices if we demand the additivity law instead of proportionality law. It is obvious from the above discussion that this corollary also holds for devices with $n \geq 4$ video device primaries whose projected color gamut onto the plane perpendicular to the color confusion axis is convex polygon with $2n$ edges.

Finally we note again that our result is not a simulation of color perception for dichromats based on human color vision mechanism but a simulation of color confusion derived from the demand on the device color gamut in computer vision algorithm.

Acknowledgments The research of HF was supported by Grant-in-Aid for Scientific Research 24500212 JSPS.

References

[1] Brettel, H., Viénot, F. and Mollon, J.D.: Computerized simulation of color appearance for dichromats, *J. Opt. Soc. Am.*, Vol.A14, pp.2647–2655 (1997).
[2] Viénot, F., Brettel, H. and Mollon, J.D.: What do colour-blind people see? *Nature*, Vol.376, pp.127–128 (1995).
[3] Dougherty, B. and Wade, A.: Vischeck, available from ⟨http://www.vischeck.com⟩.
[4] Asada, K.: Color vision tools to improve quality of life of people with color vision deficiency. Doctoral thesis, Graduate School of Media Design, Keio University, 2011.
[5] Asada, K.: Chromatic Vision Simulation, available from ⟨http://asada.tukusi.ne.jp/cvsimulation/e⟩.
[6] Capilla, P., Díez-Ajenjo, M.A., Luque, M.J. and Malo, J.: Corresponding-pair procedure: a new approach to simulation of dichromatic color perception, *J. Opt. Soc. Am.*, Vol.A21, pp.176–186 (2004).
[7] Viénot, F., Brettel, H. and Mollon, J.D.: Digital Video Colourmaps for Checking the Legibility of Displays by Dichromats, *COLOR Research and Application*, Vol.24, pp.243–252 (1999).
[8] Multimedia systems and equipment — Colour measurement and management – Part 2-1: Colour management — Default RGB colour space – sRGB, *IEC 61966-2-1 1999* (1999).
[9] Judd, D.B.: Color perceptions of deuteranopic and protanopic observations, *J. Res. Natl. Bur. stand*, Vol.41, pp.247–271 (1948).
[10] Ruddock, K.H.: Psychophysics of inherited colour vision deficiencies. in Inherited and Acquired Colour Vision Deficiencies: Fundamental Aspects and Clinical Studies, Foster, D.H. (Ed.), Vol.7 of Vision and Visual Dysfunction, pp.4–37, London, Macmillan (1991).
[11] Alpern, M., Kitahara, K. and Krantz, D.H.: Perception of colour in unilateral tritanopia, *J. Physiol.* (*London*), Vol.335, pp.683–697 (1983).
[12] Rodríguez-Pardo, C.E. and Sharma, G.: Dichromatic color perception in a two stage model: Testing for cone replacement and cone loss models, *Proc. 10th IEEE Intl. Image, Video, and Multidimensional Signal Processing Workshop: Perception and Visual Signal Analysis, Ithaca, NY, Jun. 2011*, pp.12–17 (2011).
[13] Smith, V. and Pokorny, J.: Spectral sensitivity of the foveal cone photopigments between 400 and 500 nm, *Vis Res*, Vol.15, pp.161–171 (1995).

Appendix

A.1 Simulation Function $s(Q)$ under Proportionality and Additivity Law for Exceptional Cases

We consider simulation function $\boldsymbol{s}(\boldsymbol{Q})$ under proportionality and additivity law when we cannot see three projected primary vectors in Section 4. Using notations in Section 4, since three primary vectors $\boldsymbol{E}_1, \boldsymbol{E}_2$ and $\boldsymbol{E}_3$ must be independent, at least two normalized projected vectors among $\hat{V}_1, \hat{V}_2$ and $\hat{V}_3$ are non zero. If all normalized projected vectors are non zero, it is impossible that all three normalized projected vectors are equal. Thus there are following three cases. 1) All normalized projected vectors, $\hat{V}_1, \hat{V}_2$ and $\hat{V}_3$, are non zero and all of them are non-equal. 2) All normalized projected vectors, $\hat{V}_1, \hat{V}_2$ and $\hat{V}_3$, are non zero and two of them are equal. 3) One of the normalized projected vectors, $\hat{V}_1, \hat{V}_2$ and $\hat{V}_3$, is zero. The first case is considered by the theorem 1 and the corollary 1. We show below the simulation functions $\boldsymbol{s}(\boldsymbol{Q})$'s under proportionality law in theorem 2 and 3 for the second and third case, respectively, and those under additivity law in corresponding corollaries.

Theorem 2. *When all normalized projected vectors, $\hat{V}_1, \hat{V}_2$ and $\hat{V}_3$ are non zero and two of them are equal, i.e., $\hat{V}_1 \neq 0$, $\hat{V}_2 \neq 0$, $\hat{V}_3 \neq 0$ and $\hat{V}_1 = \hat{V}_2 \neq \hat{V}_3$, the simulation function $\boldsymbol{s}(\boldsymbol{Q})$ with the properties (P1) and (P2) in the theorem 1 are determined uniquely by the simulation surface*

$$\Sigma^{(2)} = \{p(\boldsymbol{E}_1 + \boldsymbol{E}_2) + q\boldsymbol{E}_3 | p > 0, q > 0\}. \tag{A.1}$$

Proof: The parallelepiped $\boldsymbol{E}_1\boldsymbol{E}_2\boldsymbol{E}_3$ is projected to a parallelogram and two parallel edges of the parallelogram are the projections of the following two edges of the parallelepiped $\boldsymbol{E}_1\boldsymbol{E}_2\boldsymbol{E}_3$

$$\begin{aligned} e_7 &= \{t(\boldsymbol{E}_1 + \boldsymbol{E}_2) + (1-t)\boldsymbol{E}_3 | 0 \leq t \leq 1\}, \\ e_8 &= \{t\boldsymbol{E}_3 | 0 \leq t \leq 1\}. \end{aligned} \tag{A.2}$$

Since $\boldsymbol{Q}$ on e_7 and e_8 in the parallelepiped $\boldsymbol{E}_1\boldsymbol{E}_2\boldsymbol{E}_3$ has no common point with the $l_a(\boldsymbol{Q})$ except for $\boldsymbol{Q}$ itself, two edges e_7 and e_8 must be included in the simulation surface. Thus from the requirement of proportionality law the simulation surface is uniquely determined as a plane (A.1) spanned by $\boldsymbol{E}_1 + \boldsymbol{E}_2$ and $\boldsymbol{E}_3$. Q.E.D.

This is a case where one of the axes L, M or S along which dichromats cannot perceive change of color is parallel to the plane defined by the two primary vectors $\boldsymbol{E}_1$ and $\boldsymbol{E}_2$.

Corollary 2. *When all normalized projected vectors, $\hat{V}_1, \hat{V}_2$ and $\hat{V}_3$ are non zero and two of them are equal, i.e., $\hat{V}_1 \neq 0$, $\hat{V}_2 \neq 0$, $\hat{V}_3 \neq 0$ and $\hat{V}_1 = \hat{V}_2 \neq \hat{V}_3$, the simulation function $\boldsymbol{s}(\boldsymbol{Q})$ having the properties (P1) and (P3) in corollary 1 are determined uniquely by the simulation surface (A.1).*

Proof: Suppose $\boldsymbol{s}(\boldsymbol{Q})$ satisfies both (P1) and (P3) then $\boldsymbol{s}(\boldsymbol{Q})$ satisfies proportionality law as stated in Section 6. Thus by the theorem 2, $\boldsymbol{s}(\boldsymbol{Q})$ is unique and defined by the surface $\Sigma^{(p)}$ in Eq. (A.1). However the surface $\Sigma^{(p)}$ is a plane and $\boldsymbol{s}(\boldsymbol{Q})$ also satisfies additivity law. Q.E.D.

Thus for this type of special device there exists unique algorithm which simulates all colors on the device while satisfying the additivity law.

Theorem 3. *When one of the normalized projected vectors is zero, i.e., $\hat{V}_3 = 0$, the simulation function $\boldsymbol{s}(\boldsymbol{Q})$ having the properties (P1) and (P2) in theorem 1 are determined by the simulation surface*

$$\begin{aligned}
&\Sigma^{(3)} = \Sigma_5 \cup \Sigma_6 \\
&\Sigma_5 = \{p(\boldsymbol{E}_1 + r\boldsymbol{E}_2 + g(r)\boldsymbol{E}_3) | 0 \leq p \leq 1, 0 \leq r \leq 1\}, \\
&\Sigma_6 = \{p(\boldsymbol{E}_2 + (1-r)\boldsymbol{E}_1 + g(r)\boldsymbol{E}_3) | \\
&\qquad 0 \leq p \leq 1, 1 \leq r \leq 2\}, \qquad \text{(A.3)}
\end{aligned}$$

where $g(r)$ is a single-valued continuous real function defined in $0 \leq r \leq 2$ with $0 \leq g(r) \leq 1$.

Proof: The parallelepiped $\boldsymbol{E}_1\boldsymbol{E}_2\boldsymbol{E}_3$ is projected to a parallelogram and all edges of the parallelogram are the projections of the faces spanned by $\boldsymbol{E}_1$ and $\boldsymbol{E}_3$, or $\boldsymbol{E}_2$ and $\boldsymbol{E}_3$. Therefore the simulation surface is not uniquely determined and is expressed as Eq. (A.3). Q.E.D.

This is the case where one of the axes L, M or S along which dichromats cannot perceive change of color is just the primary $\boldsymbol{E}_3$.

Corollary 3. *When one of the normalized projected vectors is zero, i.e., $\hat{V}_3 = 0$, the simulation function $\boldsymbol{s}(\boldsymbol{Q})$ having the properties (P1) and (P3) in corollary 1 are determined by the simulation surface spanned by two vectors $\boldsymbol{E}_1 + g(0)\boldsymbol{E}_3$ and $\boldsymbol{E}_2 + g(2)\boldsymbol{E}_3$, where $0 \leq g(0) \leq 1$ and $0 \leq g(2) \leq 1$ are two free parameters.*

Note that in this case since simulation surface includes two free parameters $g(0)$ and $g(2)$, the simulation function $\boldsymbol{s}(\boldsymbol{Q})$ is not unique.

Hiroshi Fukuda is Associate Professor, Graduate School of Medical Sciences, Kitasato University. He received his Ph.D. in Engineering from University of Tsukuba in 1989. His research interests are Computer Vision, Discrete Geometry, and Three Body Problem. He is a member of IPSJ.

Shintaro Hara is Doctoral student, Department of Biomedical Engineering, Graduate School of Medicine, The University of Tokyo. He recieved his Master of Medical Science from Kitasato University in 2012. His research interests are Computer Vision, Computational Fluid Dynamics and Artificial Organ.

Ken asakawa is Instructor, Graduate School of Vision Science, Kitasato University. He received his Ph.D. in Ophthalmology and Vision Science from Kitasato University in 2010. His research interests are Functional evaluation and Morphological observation of Retinal Photoreceptor Cells.

Hitoshi Ishikawa is Professor, Graduate School of Medical Sciences, Kitasato University. He received his Ph.D. in Medicine from Kitasato University in 1994. His research interests are Orthoptics and Visual Science.

Makoto Noshiro received his Ph.D. in engineering from The University of Tokyo in 1981. He is currently a professor emeritus in Kitasato University. His research interests are signal processing in and identification of biomedical systems.

Mituaki Katuya is Professor Emeritus, School of Administration and Informatics, University of Shizuoka. He received his Ph.D. in Science from Hokkaido University in 1973. His research interests are Color Vision and Particle Physics.

(Communicated by *Yasutaka Furukawa*)